

The electronic contribution to the specific heat of $\text{NdBa}_2\text{Cu}_3\text{O}_{6+x}$

U. Tutsch^{1,a}, P. Schweiss², H. Wühl^{1,3}, B. Obst¹, and Th. Wolf²

¹ Forschungszentrum Karlsruhe, Institut für Technische Physik, 76021 Karlsruhe, Germany

² Forschungszentrum Karlsruhe, Institut für Festkörperphysik, 76021 Karlsruhe, Germany

³ Universität Karlsruhe, IEKP, 76128 Karlsruhe, Germany

Received 28 October 2003 / Received in final form 17 September 2004

Published online 5 November 2004 – © EDP Sciences, Società Italiana di Fisica, Springer-Verlag 2004

Abstract. From measurements of the specific heat of $\text{NdBa}_2\text{Cu}_3\text{O}_{6+x}$ in the temperature range between 20 K and 300 K the electronic contribution $C_e(T)/T$ has been derived. The results depend strongly on the assumptions made for the normal-state reference, especially the phonon contribution. Taking into account entropy conservation between the superconductor and a hypothetical normal-state reference, we found a temperature independent electronic contribution of this normal-state reference without any sign of a pseudogap for both optimum doped and underdoped samples. For oxygen concentrations between $x = 0.79$ and $x = 0.89$ a broad hump in $C_e(T)/T$ is observed around 120 K, which we ascribe to pair formation above T_c . The dependence of the hole concentration n_h in the copper oxide planes on the oxygen concentration x in the copper oxide chains was calculated by means of bond-valence sums. We found that the optimum doping of the copper oxide planes is $n_{h,opt} = 0.24$ for $R\text{Ba}_2\text{Cu}_3\text{O}_{6+x}$ ($R = \text{Nd}, \text{Y}$) irrespective of the element on the rare-earth site.

PACS. 65.40.Ba Heat capacity – 74.25.Bt Thermodynamic properties – 74.72.-h Cuprate superconductors (high- T_c and insulating parent compounds)

1 Introduction

The existence of a pseudogap in underdoped cuprate superconductors is a well known phenomenon, although its origin is still unclear. The pseudogap or effects attributed to it have been observed in many physical quantities like tunneling conductance [1,2], excitation spectra (inelastic neutron scattering [3], photoemission [4,5]), relaxation time and Knight shift [6–8], electrical resistivity [9] and the specific heat [10]. The investigation of the pseudogap by means of the specific heat makes high demands on the sample quality, the precision of the measuring equipment, and the evaluation of the data because only about 1% of the total specific heat comes from the electrons, the main contribution arising from the phonons. Loram and coworkers were the first to present results for the electronic contribution $C_e(T)/T$ to the specific heat of the $\text{YBa}_2\text{Cu}_3\text{O}_{6+x}$ system [10]. Their $C_e(T)/T$ is temperature independent in the normal state for optimum and overdoped samples, but decreases with decreasing temperature for underdoped samples. This decrease, getting

started above 200 K for $x = 0.38$ (lower end of the superconducting region in the phase diagram), was attributed to a states-non-conserving pseudogap in the normal-state-excitation spectrum [11]. The same unusual behaviour of $C_e(T)/T$ was also found in the $\text{La}_{2-x}\text{Sr}_x\text{CuO}_4$ and in the $\text{Bi}_2\text{Sr}_2\text{CaCu}_2\text{O}_{8+\delta}$ system [12]. Since the treatment of the phonon contribution highly influences the results of $C_e(T)/T$, we thought it desirable to extend these investigations to a further system in order to elucidate the difficulties arising in the analysis.

We have chosen $\text{NdBa}_2\text{Cu}_3\text{O}_{6+x}$, which is isomorphous with $\text{YBa}_2\text{Cu}_3\text{O}_{6+x}$, for two reasons: first, the variation in oxygen concentration needed to bring the system from the lower end of the superconducting region to optimum doping is smaller than in $\text{YBa}_2\text{Cu}_3\text{O}_{6+x}$ ($\delta x = 0.4$ instead of 0.55 [13,14]) suggesting a smaller change of the specific heat of the phonons in this range. Second, the tendency of the oxygen ions in the copper oxide chains to rearrange between 200 K and 300 K is smaller [15–17] so that the specific heat connected with this process is also smaller.

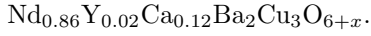
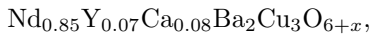
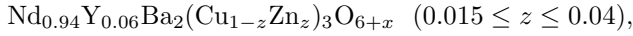
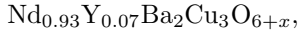
There are, however, two contributions to the specific heat of $\text{NdBa}_2\text{Cu}_3\text{O}_{6+x}$ which have no counterpart in $\text{YBa}_2\text{Cu}_3\text{O}_{6+x}$. They arise from the magnetic moments

^a e-mail: ulrich.tutsch@web.de

and the crystal-field splitted levels of the Nd^{3+} ions. Their effect on the specific heat will be discussed.

2 Experimental

High-quality single crystals were grown in SnO_2 and yttrium-stabilized ZrO_2 crucibles. The compositions, determined by neutron diffraction [18] and EDX analysis, are as follows:



No antisite defects were observed (resolution: 1% per lattice site). The small yttrium content of no more than 7% found in all but one batch (SnO_2 crucible) was due to corrosion of the ZrO_2 crucibles during the growth process and has no effect on our results. The oxygen concentrations were obtained by annealing the crystals under oxygen and oxygen/argon mixtures with oxygen partial pressures between 1 mbar and 1 bar and temperatures in the range from 280 °C to 625 °C, using the isobars of Lindemer et al. [19] as a first approximation. The exact oxygen concentrations were then determined within the framework of a complete structural analysis by neutron diffraction experiments and by gravimetry. In cases where both methods were used, a very good agreement was found, the maximum difference being $\delta x = 0.015$. The sample masses varied between 30 mg and 40 mg.

The specific heat was measured with a continuous adiabatic heating method in the temperature range from 20 K to 300 K. For each sample two warm-up rates were used, differing by a factor of two, in order to make sure that no significant heat transfer has occurred between the sample and its surroundings. The specific heat of a copper sample (27 mg) has been determined and compared with the result of a high-precision measurement in the literature [20]. The observed differences are within 1% for $T > 45$ K and 4% for $T < 45$ K. They are always positive and vary monotonically with temperature. This error is systematic and thus of no importance due to the subtraction method used here. Measuring the same sample after one year proved a reproducibility of the equipment of better than 0.2%. In the same way we obtained for the uncertainty of mass $\delta m = 0.01$ mg corresponding to a relative value of $\delta m/m = 3 \times 10^{-4}$ for the $\text{NdBa}_2\text{Cu}_3\text{O}_{6+x}$ crystals. For the oxygen concentration obtained by gravimetry and neutron diffraction an uncertainty of $\delta x = 0.015$ followed. Errors due to pieces broken off during the annealing process could be excluded since equal masses have been found at the beginning and at the end of each annealing series where the sample had the same oxygen concentration ($x \approx 1.0$).

3 Results

3.1 Specific heat

Apart from the contributions of the phonons and the electrons we expect additional contributions to the specific heat of $\text{NdBa}_2\text{Cu}_3\text{O}_{6+x}$ from the antiferromagnetically coupled copper spins in the copper oxide planes ($x < 0.55$), from the zinc ions giving rise to a Schottky-like anomaly, as well as from the spins and crystal-field-splitted levels of the Nd^{3+} ions. The specific heat of the neodymium spins does not play a part because their Néel temperature is lower than 2 K [21], which is far below our accessible temperature range (20 K–300 K). But none of the other four non-electronic contributions can be ignored. They have the following proportions compared to the electronic contribution: 100 in the case of the phonon contribution, 10 in the case of the contribution caused by the crystal-field excitations and 1 in the case of the antiferromagnetic contribution from the copper spins and the Schottky-like anomaly from the zinc ions.

Since nearly the whole specific heat is caused by the phonons, we divide the heat capacity per mol by the number of ions in the unit cell. The phonon contribution $C_{ph}(x, T)$ is then related to an effective gram-atom (gat) and should be independent of the oxygen concentration x at high temperatures. Since $\text{NdBa}_2\text{Cu}_3\text{O}_6$ is electrically insulating, the specific heat $C(0, T)$ of this compound does not contain an electronic contribution. We, therefore, use $C(0, T)$ as a first approximation for the contribution of the phonons and the crystal-field excitations, $C_{ph}(x, T) + C_{cf}(x, T)$, of $\text{NdBa}_2\text{Cu}_3\text{O}_{6+x}$ with arbitrary x . However, $\text{NdBa}_2\text{Cu}_3\text{O}_6$ is antiferromagnetically ordered below 400 K, so that $C(0, T)$ also contains an antiferromagnetic contribution $C_{af}(0, T)$ which, as far as we know, has always been regarded as negligible. To see how well $C_{ph}(x, T) + C_{cf}(x, T)$ is described by $C(0, T)$ and whether $C_{af}(0, T)$ is really negligible, the difference $\delta C(x, T)/T = C(x, T)/T - C(0, T)/T$ is shown for two oxygen concentrations in Figure 1. The main contribution to $\delta C(x, T)/T$ arises from the phonons leading to the dip-like structure with minimum around 40 K. It is caused by the increase of the Debye temperature with increasing oxygen concentration, which arises from the hardening of the crystal lattice and to a lower degree from the decrease of the mean ion mass. $\delta C_{ph}(x, T)/T$ is largest for $x = 1$ (about -15 mJ/gatK² near 40 K) but, nevertheless, an order of magnitude smaller than $C_{ph}(x, T)/T$. $\delta C_{cf}(x, T)/T$ is caused by two effects, one arising from the different numbers of ions in the unit cell to which $C_{cf}(x, T)/T$ and $C_{cf}(0, T)/T$ are referred, the other from the shift of the crystal-field-splitted levels with changing x [22, 23]. $\delta C_{cf}(x, T)/T$ has been calculated using the level values 0, 12, 20, 34 and 117 meV for $x = 1$ [22] and changing them for $x < 1$ by the same relative amount as the 34 meV level [23]. The results are in good agreement with the x dependences of the 12 and 20 meV level given in reference [22]. The calculated $\delta C_{cf}(x, T)/T$ is displayed in the inset of Figure 2. Since $\delta C_{ph}(x, T)/T$ and $\delta C_{cf}(x, T)/T$ vanish at high temperatures we expect

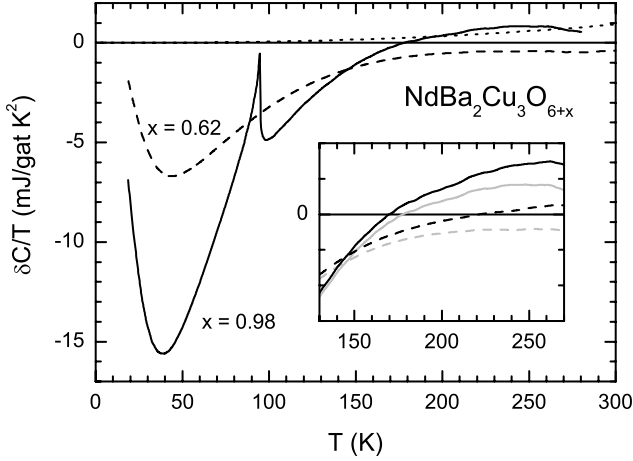


Fig. 1. Difference $\delta C(x, T)/T = C(x, T)/T - C(0, T)/T$ of the specific heat of $\text{NdBa}_2\text{Cu}_3\text{O}_{6+x}$ for $x = 0.98$ and $x = 0.62$ without correction for the antiferromagnetic contribution. The latter is described by the dotted line. The inset shows the corrected difference $\delta C(x, T)/T = C(x, T)/T - [C(0, T)/T - C_{af}(T)/T]$ (black) together with the uncorrected difference (grey) at high temperatures.

$\delta C(x, T)/T$ to approach asymptotically the electronic contribution $C_e(T)/T$ in this temperature range, provided that $C_{af}(0, T)/T$ is negligible. The fact that none of the curves in Figure 1 approaches $C_e(T)/T$, as can be seen most easily for $x = 0.62$ where $\delta C(x, T)/T$ has a negative value, points to an antiferromagnetic contribution $C_{af}(0, T)/T$ that is not negligible.

To estimate $C_{af}(0, T)/T$, we use the antiferromagnetic contribution $C_{af}^{(\text{Ru})}(T)/T$ of $\text{RuSr}_2\text{GdCu}_2\text{O}_8$, which can be extracted easier than $C_{af}(0, T)/T$ of $\text{NdBa}_2\text{Cu}_3\text{O}_6$ as its Néel temperature [24] is only 127 K, so that the antiferromagnetic anomaly is almost completely within the temperature range of our calorimeter. The procedure of determining $C_{af}^{(\text{Ru})}(T)/T$ was as follows: The specific heat of $\text{NdBa}_2(\text{Cu}, \text{Zn})_3\text{O}_7$ (normal conducting) has been used as a first approximation of the phonon background. After its subtraction $\delta C^{(\text{Ru})}/T$ remains which still contains a residual phonon and electronic contribution. The constant electronic contribution could be derived from the high-temperature behaviour of $\delta C^{(\text{Ru})}/T$ whereas the phonon contribution has been fitted using the $\delta C_{ph}/T$ curve of $\text{YBa}_2\text{Cu}_3\text{O}_7$ from [10] multiplied with a factor of 0.75 and stretched by a factor of about 1.4 along the temperature axis in order to adjust for the depth and the width of the dip in $\delta C^{(\text{Ru})}/T$. Since the RuO_2 planes and the CuO_2 planes have the same structure apart from the octahedral or pyramidal oxygen environment, their spins the same positions and the same value of 1/2, it is supposed that the antiferromagnetic contribution of $\text{NdBa}_2\text{Cu}_3\text{O}_6$ has nearly the same form as that of $\text{RuSr}_2\text{GdCu}_2\text{O}_8$. Using a Néel temperature of 385 K for $\text{NdBa}_2\text{Cu}_3\text{O}_6$ [25] and taking into account that both compounds differ in their number of ions and spins in the unit cell and that the ordered magnetic moment in $\text{NdBa}_2\text{Cu}_3\text{O}_6$ is reduced to $\mu = 0.60 \mu_B$ due to quantum fluctuations, $C_{af}(0, T)/T$ can be ob-

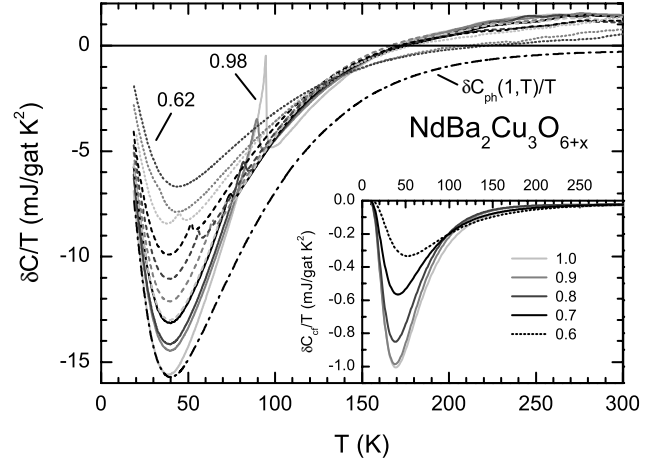


Fig. 2. Difference $\delta C(x, T)/T = C(x, T)/T - [C(0, T)/T - C_{af}(T)/T]$ of the specific heat of $\text{NdBa}_2\text{Cu}_3\text{O}_{6+x}$ after correction for the antiferromagnetic contribution for $x = 0.98, 0.94, 0.92, 0.89, 0.88, 0.84, 0.79, 0.75, 0.74, 0.70, 0.62$. Also shown is the phonon contribution $\delta C_{ph}(1, T)/T$. The inset shows $\delta C_{cf}(x, T)/T$.

tained from $C_{af}^{(\text{Ru})}(T)/T$ by two linear transformations, one for the argument and one for the function value: $C_{af}(T)/T = 2 \cdot (14/12) \cdot (0.6/1.1) \cdot C_{af}^{(\text{Ru})}((127/385)T)/T$. (The magnetic moment without fluctuations is $\mu = 1.1 \mu_B$ [26], corresponding well to the ruthenium moment $\mu^{(\text{Ru})} = 1.05 \mu_B$ of $\text{RuSr}_2\text{GdCu}_2\text{O}_8$ [27].) The corrected difference $\delta C(x, T)/T = (C(x, T) - [C(0, T) - C_{af}(T)]) / T$, shown in the inset of Figure 1 and for all oxygen concentrations in Figure 2, now approaches always a positive value at high temperatures.

Following Loram and coworkers [10] the remaining phonon contribution underlying $\delta C(x, T)/T$ can be described by:

$$\delta C_{ph}(x, T)/T = \alpha(x) \delta C_{ph}(1, T)/T, \quad 0 \leq \alpha \leq 1 \quad (1)$$

with $\alpha(x)$ to be specified. $\delta C_{ph}(1, T)/T$ is obtained by taking $\delta C(1, T)/T$ from a sample in which superconductivity has been destroyed by substituting a few percent zinc for copper and then subtracting the already mentioned Schottky-like anomaly $C_{mag}(z, T)/T$ ($z = \text{zinc concentration}$) of the zinc-doped samples as well as the contribution from the crystal-field excitations $\delta C_{cf}(x, T)/T$ and the electronic contribution $C_e(T)/T$. $C_{mag}(z, T)/T$ possibly arises from antiferromagnetically ordered copper spins around the zinc ions [28] and has its maximum at about 20 K reaching values of the same magnitude as the electronic contribution. We could determine $C_{mag}(z, T)/T$ by comparing the specific heat of samples with different zinc but similar oxygen concentrations. Since a temperature independent electronic contribution $C_e(T)/T = \gamma$ has been observed in $\text{YBa}_2(\text{Cu}_{0.93}\text{Zn}_{0.07})_3\text{O}_{6.97}$ [10], we take this result for $\text{NdBa}_2(\text{Cu}, \text{Zn})_3\text{O}_7$ and obtain γ by extrapolating $\delta C(1, T)/T$ with a $1/T^3$ function (according to the high-temperature behaviour of the difference between to Einstein specific heat functions) to $T = \infty$.

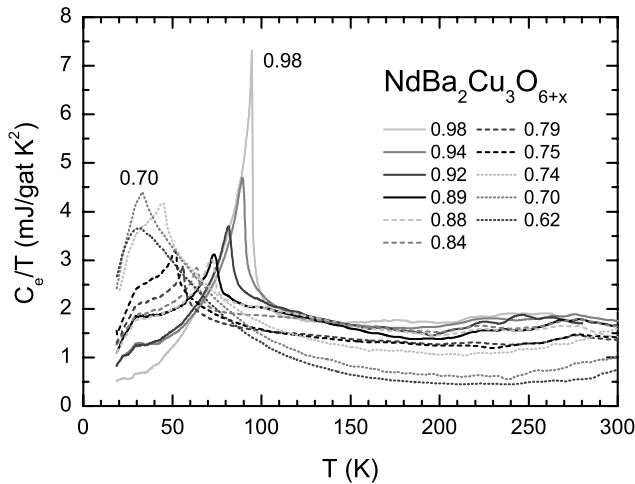


Fig. 3. First approximation for the electronic specific heat $C_e(T)/T$ of $\text{NdBa}_2\text{Cu}_3\text{O}_{6+x}$ using the phonon contribution $\alpha(x)\delta C_{ph}(1, T)/T$ with a linear interpolation between $\alpha(0) = 0$ and $\alpha(1) = 1$.

The result for $\delta C_{ph}(1, T)/T$ is shown in Figure 2 by the black dash-dotted line.

Assuming as a first approximation $\alpha(x) = x$, it follows for the electronic specific heat:

$$C_e(x, T)/T = \delta C(x, T)/T - x\delta C_{ph}(1, T)/T - \delta C_{cf}(x, T)/T. \quad (2)$$

The results are shown in Figure 3. Obviously, the broad peak at 40 K occurring in $C_e(T)/T$ for lower x values ($x \leq 0.74$) is an artifact. As its shape is similar to the shape of the dip in $\delta C_{ph}(1, T)/T$ (see Fig. 2), it is very likely that it results from a remaining phonon contribution. Apparently, the function $\delta C_{ph}(1, T)/T$ alone is not sufficient to describe the phonon contribution for all x values. Since we want to derive $C_e(T)/T$ only for oxygen concentrations between $x = 0.62$ and $x = 1$, we narrow the interpolation range by raising its lower bound from $x = 0$ to 0.62. We do this by determining $\delta C_{ph}(0.62, T)/T$ in the same way as $\delta C_{ph}(1, T)/T$ (but without using a zinc-doped reference since the sample is still non-superconducting) and then interpolating linearly between $\delta C_{ph}(1, T)/T$ and $\delta C_{ph}(0.62, T)/T$:

$$\delta C_{ph}(x, T)/T = \alpha(x)\delta C_{ph}(1, T)/T + (1 - \alpha(x))\delta C_{ph}(0.62, T)/T, \quad 0 \leq \alpha \leq 1. \quad (3)$$

The assumption of a temperature independent electronic contribution $C_e(0.62, T)/T$, which we made to extract $\delta C_{ph}(0.62, T)/T$ out of $\delta C(0.62, T)/T$, does not affect our results for $C_e(x, T)/T$ since $C_e(0.62, T)/T$ is so small (0.44 mJ/gatK² in the extrapolation $T \rightarrow \infty$) that it does not play a part even if it would decrease with decreasing temperature, as is the case for a states-non-conserving pseudogap.

Figure 4 shows the results for $C_e(x, T)/T$ after subtraction of the phonon contribution described by equation (3) with $\alpha(x) = x$. The broad peaks at 40 K

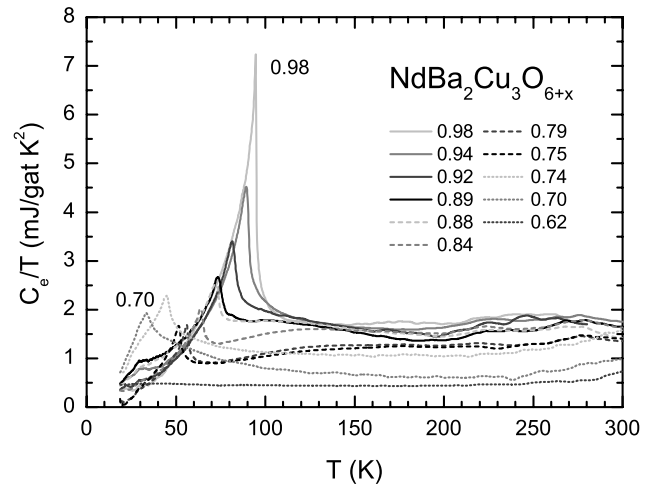


Fig. 4. Second approximation for the electronic specific heat $C_e(T)/T$ of $\text{NdBa}_2\text{Cu}_3\text{O}_{6+x}$ using the phonon contribution $\alpha(x)\delta C_{ph}(1, T)/T + (1 - \alpha(x))\delta C_{ph}(0.62, T)/T$ with a linear interpolation between $\alpha(0.62) = 0$ and $\alpha(1) = 1$.

in Figure 3 now have vanished. Besides the superconducting anomaly, broadened by thermal fluctuations [29], a broad hump becomes apparent above T_c followed by the already mentioned contribution due to the oxygen rearrangement above 200 K. For $\text{NdBa}_2\text{Cu}_3\text{O}_{6.94}$ this contribution to the specific heat is only 1/4 of that we found for $\text{YBa}_2\text{Cu}_3\text{O}_{6.95}$, which is in good agreement with results from thermal expansion experiments [15–17]. The smaller contribution of the oxygen rearrangement process is an essential advantage for the next step of the evaluation of $C_e(T)/T$ in $\text{NdBa}_2\text{Cu}_3\text{O}_{6+x}$.

The change in sign of the slope of $C_e(T)/T$ above T_c at low doping in Figure 4 suggests a still not quite correct treatment of the phonon contribution. We therefore drop the approximation $\alpha(x) = x$ in equation (3) and permit a slight deviation from the linear dependence. For the new determination of $\alpha(x)$ we use entropy conservation between the superconductor and the normal-state reference into which the superconductor would change if superconductivity would be suppressed. This (hypothetical) normal-state reference has to be determined.

The broad hump above T_c is supposed to be a property of the superconductor, possibly arising from the formation of pairs within charge stripes [30], and thus should not appear in the electronic contribution $C_{en}(T)/T$ of the normal-state reference. At 200 K the contribution of the hump has become rather small and the oxygen rearrangement process has not yet set in. Therefore, we can use $C_e(T)/T$ at this temperature as starting-point for $C_{en}(T)/T$.

Surprisingly, it is for a temperature independent $C_{en}(T)/T = \gamma$ that we always find an $\alpha(x)$ so that the superconducting sample has the same entropy $S = \int_0^{200\text{K}} C_e(T)/T dT$ as the normal-state reference. (Below 20 K $C_e(T)/T$ was extrapolated towards $T = 0$ with $\gamma_0 + aT^n$, $\gamma_0 = 0$ for x values below the 60 K plateau and ≈ 0.2 above.) The resulting $C_e(T)/T$ is plotted in Figure 5.

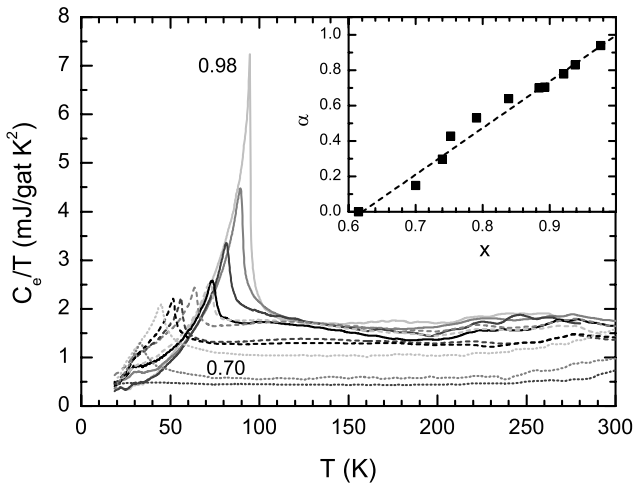


Fig. 5. Final result for the electronic specific heat $C_e(T)/T$ of $\text{NdBa}_2\text{Cu}_3\text{O}_{6+x}$ using the phonon contribution $\alpha(x)\delta C_{ph}(1, T)/T + (1 - \alpha(x))\delta C_{ph}(0.62, T)/T$ with a non-linear interpolation between $\alpha(0.62) = 0$ and $\alpha(1) = 1$. The inset shows $\alpha(x)$.

The temperature independent behaviour of the underlying $C_{en}(T)/T$ is obvious. The inset shows the small correction made for $\alpha(x)$ to assure entropy conservation. If we had allowed $C_{en}(T)/T$ to decrease with decreasing temperature for more than 30% of its value at 200 K, entropy conservation would not have been possible. The large decrease of $C_e(T)/T$ with decreasing temperature already starting above 200 K which has been observed by Loram and coworkers in $\text{YBa}_2\text{Cu}_3\text{O}_{6+x}$ [10] cannot be confirmed by our investigations on $\text{NdBa}_2\text{Cu}_3\text{O}_{6+x}$.

The features in $C_e(T)/T$ characteristic for intermediate oxygen concentrations are enlarged in Figure 6. Besides the fluctuation broadened superconducting transition, the broad hump centered at about 120 K is clearly visible. It is followed by the contribution of the oxygen rearrangement process showing a double structure, which is also seen in the thermal expansion [17].

The specific heat of the $\text{Nd}_{1-y}\text{Ca}_y\text{Ba}_2\text{Cu}_3\text{O}_{6+x}$ samples has been analyzed in the same way as for $\text{NdBa}_2\text{Cu}_3\text{O}_{6+x}$. The result for 12% calcium-doped crystals is shown in Figure 7. Since the substitution of calcium for neodymium is alternative to oxygen charging as far as the supply of the copper oxide planes with holes is concerned, similar results are obtained at smaller oxygen concentrations.

3.2 Hole concentration

In order to present characteristic quantities of the electronic specific heat in dependence on the hole concentration in the copper oxide planes, the hole distribution in the unit cell was calculated for different oxygen concentrations x by means of bond-valence sums from our structural data determined by elastic neutron scattering. We present these calculations in some detail, since we clearly

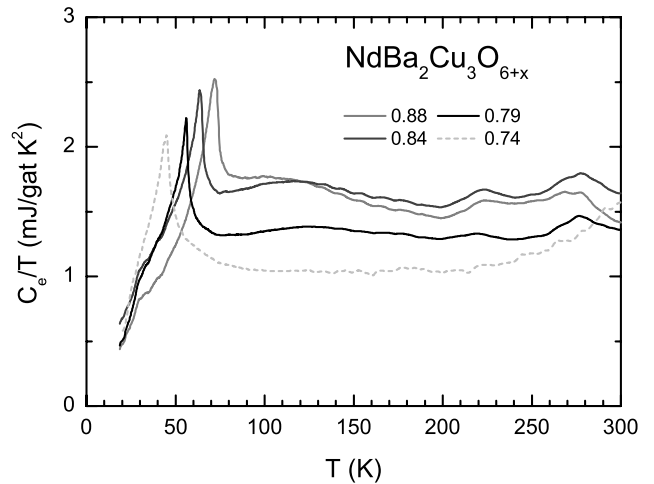


Fig. 6. Electronic specific heat $C_e(T)/T$ of $\text{NdBa}_2\text{Cu}_3\text{O}_{6+x}$ from Figure 5 for oxygen concentrations showing the hump. $C_e(T)/T$ for $x = 0.74$ serves as a reference without a hump.

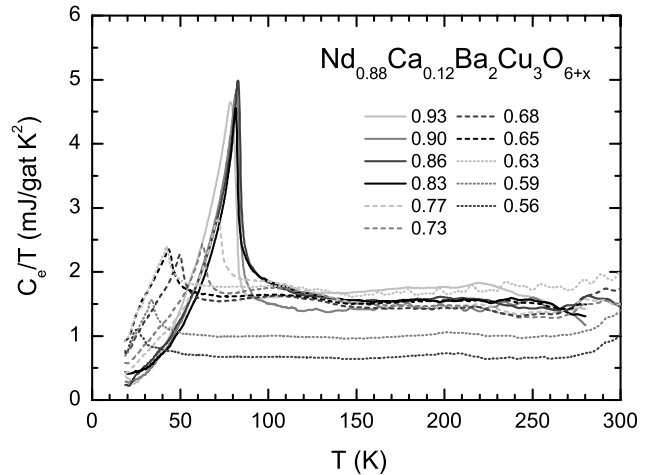


Fig. 7. Electronic specific heat $C_e(T)/T$ of $\text{Nd}_{0.88}\text{Ca}_{0.12}\text{Ba}_2\text{Cu}_3\text{O}_{6+x}$. The phonon contribution has been determined in the same way as in Figure 5.

obtain higher values than the commonly used values originating from calculations by Tallon [31]. As described by Brown and Altermatt [32–34] the charge of an ion is represented by a sum of bond valences with its next neighbours of opposite charge sign according to $V_i = \sum_j s_{ij}$, with $s_{ij} = \exp((R_{ij} - d_{ij})/0.37\text{\AA})$ depending exponentially on the distance d_{ij} between the ions i and j and a constant R_{ij} characteristic for this ion pair. A correction of the ion charges due to internal stress is most essential. This correction can be easily performed for the non-copper ions because their charges are integers. However, since the copper ions do not have integer valences and, moreover, occupy different kinds of lattice sites (planes, chains) a simple way of getting their charge corrections does not exist. According to Brown we assume these charge corrections to be the same for all copper ions leading to physically plausible results at $x = 0$. Therefore, we regard this assumption as a sufficiently good approximation. Since in

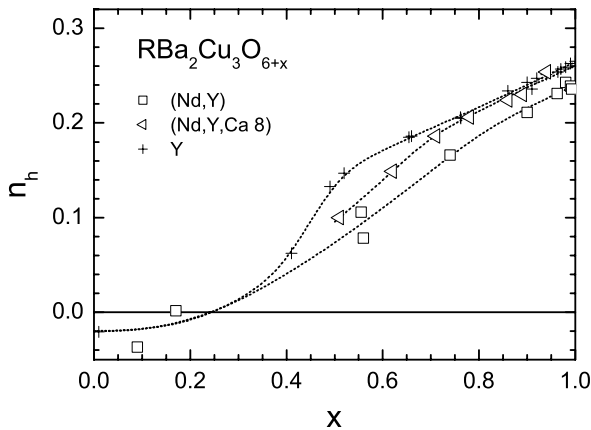


Fig. 8. Hole concentration n_h of the copper oxide planes for $\text{RBa}_2\text{Cu}_3\text{O}_{6+x}$ as function of the oxygen concentration x .

our calculations the holes reside on the copper sites, they still have to be redistributed over the oxygen ions where they are experimentally found. This can be simply done by adjusting R_{CuO} as described in [33].

The resulting $n_h(x)$ dependences are shown in Figure 8. The results obtained for $(\text{Nd}, \text{Y})\text{Ba}_2\text{Cu}_3\text{O}_{6+x}$ are also used for $\text{NdBa}_2\text{Cu}_3\text{O}_{6+x}$. In the case of $(\text{Nd}, \text{Y})_{0.88}\text{Ca}_{0.12}\text{Ba}_2\text{Cu}_3\text{O}_{6+x}$ the results of $(\text{Nd}, \text{Y})_{0.92}\text{Ca}_{0.08}\text{Ba}_2\text{Cu}_3\text{O}_{6+x}$ were used taking into account the higher calcium content. This procedure is justified because of the small differences in the yttrium content and in the case of the calcium doped samples additionally by one reference point at about $x = 0.6$. In contrast to the widely used value of 0.16 for optimum doping [31] where T_c shows its maximum ($T_{c,\text{max}}$), we obtained $n_{h,\text{opt}} = 0.24$ for both $\text{NdBa}_2\text{Cu}_3\text{O}_{6+x}$ and $\text{YBa}_2\text{Cu}_3\text{O}_{6+x}$. Our results are in good agreement with those of Brown [33,34] and more precise results recently published by Eckstein and Kuper [35]. Moreover, they are experimentally supported by X-ray absorption spectroscopy of Merz et al. [36]. The disregard of stress corrections and the application of inconsistent R_{CuO} values are the main reason why Tallon's n_h values [31] deviate from ours. Since beyond any doubt the $\text{La}_{2-x}\text{M}_x\text{CuO}_4$ ($M = \text{Ba}, \text{Sr}$) system is optimally doped at $n_{h,\text{opt}} = 0.16$, the higher value $n_{h,\text{opt}} = 0.24$ of the $\text{RBa}_2\text{Cu}_3\text{O}_{6+x}$ ($R = \text{Nd}, \text{Y}$) family shows that for cuprate superconductors a universal dependence of $T_c/T_{c,\text{max}}$ on the hole concentration in the planes holds only if the normalized parameter $n_h/n_{h,\text{opt}}$ is used.

4 Discussion

In Figure 9 the normalized transition temperature $T_c/T_{c,\text{max}}$, the Sommerfeld coefficient $\gamma = C_{\text{en}}(T)/T$, and the mean-field jump $\Delta C/T_c^{(\text{mf})}$ of the specific heat are plotted as functions of the hole concentration n_h per copper oxide plane. T_c is taken at the maximum of the specific heat anomaly, γ at about 200 K where the rearrangement process of the oxygen ions has not yet set in, and

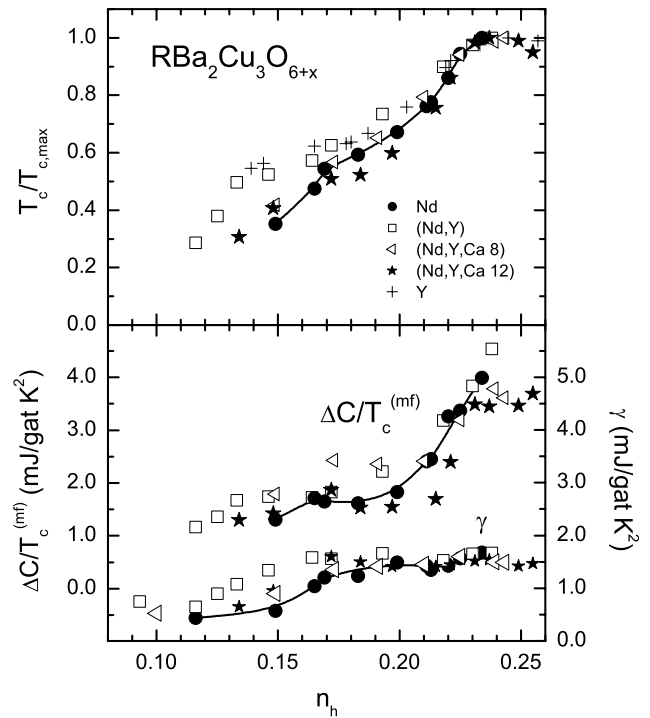


Fig. 9. Normalized transition temperature $T_c/T_{c,\text{max}}$, jump $\Delta C/T_c^{(\text{mf})}$ of the specific heat, and Sommerfeld coefficient γ for the compounds $\text{NdBa}_2\text{Cu}_3\text{O}_{6+x}$, $(\text{Nd}, \text{Y})\text{Ba}_2\text{Cu}_3\text{O}_{6+x}$, $(\text{Nd}, \text{Y})_{0.92}\text{Ca}_{0.08}\text{Ba}_2\text{Cu}_3\text{O}_{6+x}$, and $(\text{Nd}, \text{Y})_{0.88}\text{Ca}_{0.12}\text{Ba}_2\text{Cu}_3\text{O}_{6+x}$. The T_c values of $\text{YBa}_2\text{Cu}_3\text{O}_{6+x}$ are from reference [37]. Note that our n_h values are roughly a factor of 1.5 larger than the commonly used n_h values.

$\Delta C/T_c^{(\text{mf})}$ is obtained by constructing (entropy conserving) a mean-field jump at $T_c^{(\text{mf})} > T_c$ from the fluctuation broadened superconducting anomaly. As expected, each of these quantities is independent of the chemical composition of this cuprate family, when plotted as function of n_h .

The transition temperature shows a dip in $T_c(n_h)$ similar to the so-called 60 K plateau in the $T_c(x)$ -dependence. In the case of $\text{YBa}_2\text{Cu}_3\text{O}_{6+x}$, the 60 K plateau has usually been attributed to oxygen ordering in the copper oxide chains. The results of Figure 9, however, speak for an intrinsic property of the copper oxide planes. From this point of view the origin of the dip in $T_c(n_h)$ could be the same as for $\text{La}_{2-x}\text{Ba}_x\text{CuO}_4$ and $\text{La}_{1.6-x}\text{Nd}_{0.4}\text{Sr}_x\text{CuO}_4$, where superconductivity even vanishes completely at $x \approx 0.12$ ($n_h \approx 1/8$). In $\text{La}_{1.48}\text{Nd}_{0.4}\text{Sr}_{0.12}\text{CuO}_4$ the collapse of T_c has been attributed to static spin-charge stripes, which have been observed in neutron scattering experiments [38]. But the formation of static stripes has never been observed unambiguously in $\text{YBa}_2\text{Cu}_3\text{O}_{6+x}$. The recent observation of modulations in the spin susceptibility of highly ordered $\text{YBa}_2\text{Cu}_3\text{O}_{6.5}$ [39] points to the existence of dynamic stripes. An only weak pinning of the stripes could be the reason for the relatively weak T_c suppression around $n_h = 0.20$.

In the model of Emery and coworkers [30] dynamic spin-charge stripes develop below the upper pseudogap

temperature T_1^* which merges in $T_c(n_h)$ in the overdoped region and increases steeply with decreasing n_h . Within the charge stripes incoherent hole pairing develops at the lower pseudogap temperature T_2^* which also merges in $T_c(n_h)$ in the overdoped region but remains almost constant in the underdoped region. We have associated the hump in our $C_e(T)/T$ data above T_c with this pairing. Its maximum roughly coincides with T_2^* . The hump is most pronounced for $x = 0.84$ corresponding to $n_h = 0.20$, where $T_c(n_h)$ has its dip. At lower hole concentrations the hump is expected to decrease as γ decreases and at higher hole concentrations it may merge into a BCS-like anomaly at T_c .

The spin-charge separation below T_1^* does not become evident as pseudogap in our results. The temperature independent $C_{en}(T)/T$ in the whole doping range is not in line with a $C_{en}(T)/T$ decreasing with decreasing temperature as claimed by Loram and coworkers in the case of underdoped YBa₂Cu₃O_{6+x}. The hump in $C_e(T)/T$ above T_c , however, is also visible in their results. In our picture of preformed pairs within charge stripes, the decrease of $\Delta C/T_c^{(mf)}$ in the n_h range where T_c collapses is caused by restricted dynamics of the stripes. Indeed, $\Delta C/\gamma T_c^{(mf)}$, which is a measure of the superconducting coupling strength, exhibits a minimum around $n_h = 0.18$ and reaches nearly the same coupling strength at $n_h = 0.15$ as at optimum doping. This explanation is supported by a peak in the pressure effect dT_c/dp in the same doping range, which has been attributed to depinning of stripes [40].

In conclusion, we have revealed how sensitively the extraction of the electronic contribution $C_e(T)/T$ from the total specific heat depends on the assumptions made for the normal-state reference, especially the phonon contribution $C_{ph}(T)/T$. Using rigorously entropy conservation between the superconductor and a hypothetical normal-state reference, we obtain a $C_e(T)/T$ characterized by a fluctuation broadened superconducting transition followed by a hump, which is attributed to pair formation within the charge stripes. The underlying electronic contribution $C_{en}(T)/T$ of the normal state is temperature independent for both optimum and underdoped samples and does not indicate the existence of a pseudogap. In addition, we found that a generic phase diagram (with a dip in $T_c(n_h)$) for cuprate superconductors only exists if the normalized parameter $n_h/n_{h,opt}$ is used. For the $R\text{Ba}_2\text{Cu}_3\text{O}_{6+x}$ system ($R = \text{Nd}, \text{Y}$) we claim $n_{h,opt} = 0.24$ for optimum doping in contrast to the generally used $n_{h,opt} = 0.16$, which is certainly correct for the $\text{La}_{2-x}\text{M}_x\text{CuO}_4$ system ($M = \text{Ba}, \text{Sr}$).

References

- H.J. Tao, F. Lu, E.L. Wolf, *Physica C* **282-287**, 1507 (1997)
- Ch. Renner, B. Revaz, J.-Y. Genoud, K. Kadowaki, Ø. Fischer, *Phys. Rev. Lett.* **80**, 149 (1998)
- J. Rossat-Mignod, L.P. Regnault, C. Vettier, P. Bourges, P. Burllet, J. Bossy, J.Y. Henry, G. Lapertot, *Physica C* **185-189**, 86 (1991)
- H. Ding, T. Yokoya, J.C. Campuzano, T. Takahashi, M. Randeria, M.R. Norman, T. Mochiku, K. Kadowaki, J. Giapintzakis, *Nature* **382**, 51 (1996)
- A.G. Loeser, Z.-X. Shen, D.S. Dessau, D.S. Marshall, C.H. Park, P. Fournier, A. Kapitulnik, *Science* **273**, 325 (1996)
- W.W. Warren, Jr., R.E. Walstedt, G.F. Brennert, R.J. Cava, R. Tycko, R.F. Bell, G. Dabbagh, *Phys. Rev. Lett.* **62**, 1193 (1989)
- R.E. Walstedt, W.W. Warren, Jr., R.F. Bell, R.J. Cava, G.P. Espinosa, L.F. Schneemeyer, J.V. Waszczak, *Phys. Rev. B* **41**, 9574 (1990)
- M. Takigawa, A.P. Reyes, P.C. Hammel, J.D. Thompson, R.H. Heffner, Z. Fisk, K.C. Ott, *Phys. Rev. B* **43**, 247 (1991)
- B. Batlogg, H.Y. Hwang, H. Takagi, R.J. Cava, H.L. Kao, J. Kwo, *Physica C* **235-240**, 130 (1994)
- J.W. Loram, K.A. Mirza, J.R. Cooper, W.Y. Liang, *Phys. Rev. Lett.* **71**, 1740 (1993)
- J.W. Loram, K.A. Mirza, J.M. Wade, J.L. Tallon, *Physica C* **235-240**, 1735 (1994)
- J.W. Loram, J. Luo, J.R. Cooper, W.Y. Liang, J.L. Tallon, *J. Phys. Chem. Solids* **62**, 59 (2001)
- H. Lütgemeier, S. Schmenn, P. Meuffels, O. Storz, R. Schöllhorn, Ch. Niedermayer, I. Heinmaa, Yu. Baikov, *Physica C* **267**, 191 (1996)
- G. Flor, G. Chiodelli, G. Spinolo, P. Ghigna, *Physica C* **316**, 13 (1999)
- P. Nagel, V. Pasler, C. Meingast, A.I. Rykov, S. Tajima, *Phys. Rev. Lett.* **85**, 2376 (2000)
- P. Nagel, *Wissenschaftliche Berichte FZKA 6661*, Forschungszentrum Karlsruhe (2001)
- H. Leibrock, *Wissenschaftliche Berichte, FZKA 6819*, Forschungszentrum Karlsruhe (2003)
- neutron diffraction experiments at the four-circle diffractometer 5C₂ at the Orphée reactor, Laboratoire Léon Brillouin, Laboratoire commun CEA-CNRS, CE Saclay
- T.B. Lindemer, E.D. Specht, P.M. Martin, M.L. Flitcroft, *Physica C* **255**, 65 (1995)
- D.L. Martin, *Rev. Sci. Instrum.* **58**, 639 (1987)
- K.N. Yang, J.M. Ferreira, B.W. Lee, M.B. Maple, W.-H. Li, J.W. Lynn, R.W. Erwin, *Phys. Rev. B* **40**, 10963 (1989)
- H. Dröbner, H.-D. Jostarndt, J. Harnischmacher, J. Kalenborn, U. Walter, A. Severing, W. Schlabit, E. Holland-Moritz, *Z. Phys. B* **100**, 1 (1996)
- A.A. Martin, T. Ruf, T. Strach, M. Cardona, Th. Wolf, *Phys. Rev. B* **58**, 14349 (1998)
- J.W. Lynn, B. Keimer, C. Ulrich, C. Bernhard, J.L. Tallon, *Phys. Rev. B* **61**, R14964 (2000)
- A.H. Moudden, G. Shirane, J.M. Tranquada, R.J. Birgeneau, Y. Endoh, K. Yamada, Y. Hidaka, T. Murakami, *Phys. Rev. B* **38**, 8720 (1988)
- A. Abragam, B. Bleaney, *Electron Paramagnetic Resonance of Transition Ions* (Clarendon Press, Oxford, 1970), p. 459
- C. Bernhard, J.L. Tallon, Ch. Niedermayer, Th. Blasius, A. Golnik, E. Brücher, R.K. Kremer, D.R. Noakes, C.E. Stronach, E.J. Ansaldo, *Phys. Rev. B* **59**, 14099 (1999)
- C.-S. Jee, D. Nichols, A. Kebede, S. Rahman, J.E. Crow, A.M. Ponte Goncalves, T. Mihalisin, G.H. Myer, I. Perez, R.E. Salomon, P. Schlottmann, S.H. Bloom, M.V. Kuric, Y.S. Yao, R.P. Guertin, *J. Supercond.* **1**, 63 (1988)
- C. Meingast, V. Pasler, P. Nagel, A. Rykov, S. Tajima, P. Olsson, *Phys. Rev. Lett.* **86**, 1606 (2001)

30. V.J. Emery, S.A. Kivelson, O. Zacher, Phys. Rev. B **56**, 6120 (1997); E.W. Carlson, V.J. Emery, S.A. Kivelson, D. Orgad, *cond-mat/0206217* v1 (2002)
31. J.L. Tallon, Physica C **168**, 85 (1990)
32. I.D. Brown, D. Altermatt, Acta Cryst. B **41**, 244 (1985)
33. I.D. Brown, J. Solid State Chem. **82**, 122 (1989)
34. I.D. Brown, J. Solid State Chem. **90**, 155 (1991)
35. Y. Eckstein, C.G. Kuper, Physica B **284-288**, 403 (2000)
36. M. Merz, N. Nücker, P. Schweiss, S. Schuppler, C.T. Chen, V. Chakarian, J. Freeland, Y.U. Idzerda, M. Kläser, G. Müller-Vogt, Th. Wolf, Phys. Rev. Lett. **80**, 5192 (1998)
37. S. Schlachter, diploma thesis, University of Karlsruhe (1997), p. 36
38. J.M. Tranquada, B.J. Sternlieb, J.D. Axe, Y. Nakamura, S. Uchida, Nature **375**, 561 (1995)
39. C. Stock, W.J.L. Buyers, R. Liang, D. Peets, Z. Tun, D. Bonn, W.N. Hardy, R.J. Birgeneau, Phys. Rev. B **69**, 014502 (2004)
40. S.I. Schlachter, U. Tutsch, W.H. Fietz, K.-P. Weiss, H. Leibrock, K. Grube, Th. Wolf, B. Obst, P. Schweiss, H. Wühl, Int. J. Mod. Phys. B **14**, 3673 (2000)